JOC The Journal of Organic Chemistry

ARTICLE

pubs.acs.org/joc

Kinetic Analysis of the Phenyl-Shift Reaction in β-O-4 Lignin Model Compounds: A Computational Study

Ariana Beste*,† and A. C. Buchanan, III‡

†Joint Institute of Computational Sciences, Oak Ridge National Laboratory, Oak Ridge, Tennessee 37831, United States

‡Chemical Sciences Division, Oak Ridge National Laboratory, Oak Ridge, Tennessee 37831, United States

Supporting Information

ABSTRACT:

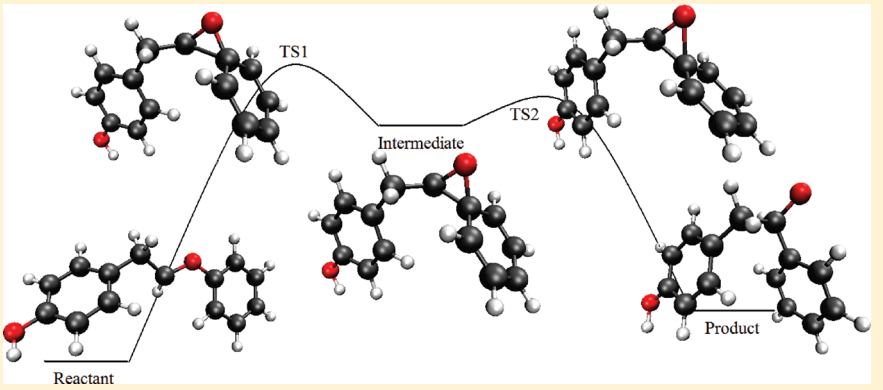

The phenyl-shift reaction for the β-radical of phenethyl phenyl ether ($PhCH_2\dot{C}HOPh$, β-PPE) is an integral step in the pyrolysis of PPE, which is a model compound for the β-O-4 linkage in lignin. We investigated the influence of natural occurring substituents (hydroxy, methoxy) on the reaction rate by calculating relative rate constants using density functional theory in combination with transition state theory, including anharmonic correction for low-frequency modes. The phenyl-shift reaction proceeds through an oxaspiro[2.5]octadienyl radical intermediate and the overall rate constants were computed invoking the steady-state approximation (its validity was confirmed). Substituents on the phenethyl ring have only little influence on the rate constants. If a methoxy substituent is located in the para position of the phenyl ring adjacent to the ether oxygen, the energies of the intermediate and second transition state are lowered, but the overall rate constant is not significantly altered. This is a consequence of the dominating first transition from reactant to intermediate in the overall rate constant. In contrast, *o*- and di-*o*-methoxy substituents significantly accelerate the phenyl-migration rate compared to β-PPE.

1. INTRODUCTION

The development of clean technologies for the production of fuels and chemicals has become a focal point of research activities. Biomass is a promising resource for valuable chemicals and fuels.[1−6] Even though lignin can account for up to one-third of biomass, most industrially accessible lignin is consumed as fuel with little alternative large-scale application. This is due to the complexity and the chemical stability of lignin, which requires harsh reaction conditions for its depolymerization. Another complicating factor is that the composition and structural attributes of lignin depend on cell tissue and plant species. For these reasons, the mechanistic study of lignin conversion is very difficult. Often, model compounds, representing the various linkages and substituent distributions in lignin, are investigated instead. The β-O-4 linkage is by far the most common linkage and much research has been dedicated to it.[7−13]

The simplest model for the β-O-4 linkage in lignin is phenethyl phenyl ether ($PhCH_2CH_2OPh$, PPE). Depending on the reaction conditions (temperature, solvent, concentration, heating rate, pH), multiple mechanisms might be relevant for its thermal decomposition. However, at moderate temperatures (603−698 K) and conventional pyrolysis conditions, a free radical chain mechanism, shown in Scheme 1, is consistent with experimental data. Britt et al.[14] studied the pyrolysis of PPE in the neat liquid, in solution, and in the gas phase and found that the thermolysis of PPE proceeds through two competitive pathways, defined as α/β-selectivity. PhOH + $PhCH{=}CH_2$ forms through the α-channel and PhCHO + $PhCH_3$ through the β-channel. The rate determining reaction steps are the hydrogen abstraction reactions 2 and 6. Hydrogen abstraction is typically followed by β-scission. Whereas the β-scission of the α-radical (reaction 3) is fast, possible β-scission steps for the β-radical are slow and intermolecular hydrogen abstraction can potentially convert

Received: January 6, 2011
Published: March 07, 2011

 © 2011 American Chemical Society

Scheme 1. Radical Chain Mechanism for the Pyrolysis of PPE[a]

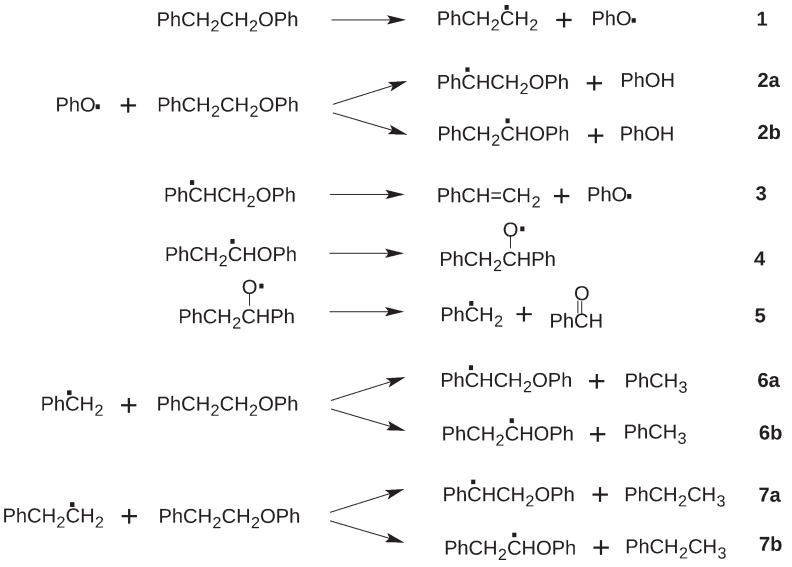

[a] At 375 °C, the chain length is approximately 30−35 cycles long, where termination is predominantly caused by benzyl radical coupling.[14]

the β- into the α-radical, thereby increasing the selectivity of thermal decomposition. However, if 1,2 phenyl migration is sufficiently fast (reaction 4), radical interconversion is suppressed since the β-scission of the migration product (reaction 5) is again fast.

In subsequent work, Britt et al. studied the influence of naturally occurring oxygen substituents on the pyrolysis mechanism of PPE.[15] Substituents can perturb all key steps in the mechanism, as well as the kinetic chain length, and are difficult to analyze experimentally. An advantage of computational methods is the ability to investigate individual reaction steps and evaluate the effect of substituents on intermediate stages of the reaction process separately. Density functional theory (DFT) has been used to study various aspects of lignin model chemistry, such as β-scission of the α-PPE radical,[9] the characterization of active sites in monolignols,[16] and the addition of monolignols.[17] Higher level methods have been applied to calculate enthalpies of reaction for the homolytic cleavage of PPE,[18] to study the intramolecular hydrogen bond in the guaiacyl structural unit,[19] and to investigate the pyrolysis of *o*-quinone methide.[20]

In previous work, we used DFT to examine substituent effects on the initiation reaction of the pyrolysis mechanism of PPE (reaction 1)[21] and to explore the influence of the substituents on the relative rate constants of hydrogen abstraction (reactions 2 and 6).[22−24] Overall α/β-selectivities can be derived from forward rate constants of hydrogen abstraction alone[22,23] if the steady-state approximation for the intermediates is applicable and the interconversion between α- and β-PPE radicals is slow compared to phenyl migration. Otherwise, overall rates and product distributions can only be obtained by integration of the rate equations considering all reactions participating in the pyrolysis mechanism. Substituents play a vital role in the determination of a suitable kinetic model; i.e. if methoxy substituents are located on the phenyl ring adjacent to the ether oxygen,[24] reverse hydrogen abstraction has to be considered making a complete numerical model necessary.

In the following, we present our study on the phenyl migration (Scheme 1, reaction 4), where naturally occurring substituents (hydroxy, methoxy) are introduced on either phenyl ring of PPE. Reaction 4 is not only a critical step in the thermolysis process for β-O-4 lignin models, but is also of general interest. It is very similar to the reverse reaction of a neophyl-like rearrangement, where an oxygen-centered radical is converted into a carbon-centered radical through a phenyl shift. Researchers had opposing opinions on whether the reaction proceeds through an intermediate[25,26] or transition state,[27] with recent DFT studies supporting the existence of a reactive intermediate.[28,29] Our work provides new insights into another member of this reaction family, including the influence of key substituents on the reaction rates.

Scheme 2. β-Radicals of PPE and PPE Derivatives Investigated in This Work

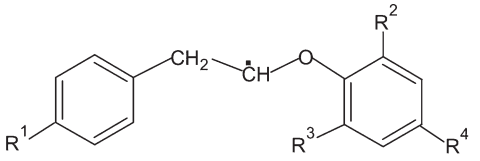

1 R^1,R^2,R^3,R^4=H
2 R^1=OH,R^2,R^3,R^4=H
3 R^1=OCH_3,R^2,R^3,R^4=H
4 R^1,R^2,R^3=H,R^4=OCH_3
5 R^1=H,R^2=OCH_3,R^3,R^4=H
6 R^1=H,R^2,R^3=OCH_3,R^4=H

2. RESULTS AND DISCUSSION

We investigated the phenyl-shift reaction 4 in β-radicals of PPE derivatives, which are shown in Scheme 2. The β-radicals are produced from PPE through hydrogen abstraction. Various conformers of PPE derivatives **1**, **4**, **5**, and **6** were determined with the M06-2X functional[30] and have been discussed in previous work,[24] which focused on hydrogen abstraction steps. Reaction profiles in this work show the energies of the reactant conformers that were obtained as the energetically lowest

dx.doi.org/10.1021/jo2000385 |*J. Org. Chem.* 2011, 76, 2195–2203

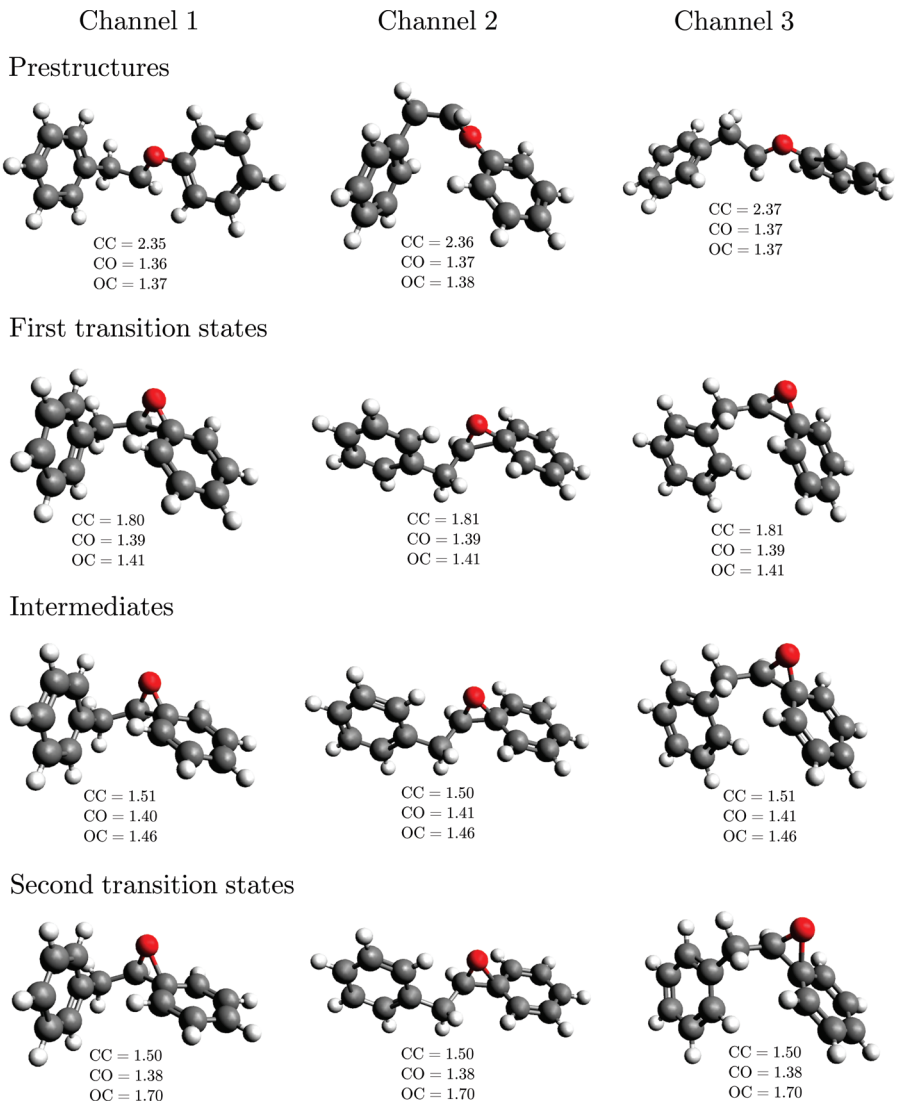

Figure 1. Prestructures, first transition states, intermediates, and second transition states for the reaction channels of the phenyl migration in the β-PPE radical; bond distances in Å; CC, carbon−carbon bond in the epoxy group; CO, aliphatic carbon−oxygen bond in the epoxy group; OC, oxygen-aromatic carbon in the epoxy group.

product of hydrogen abstraction; their structures are given in the Supporting Information. Products correspond to the next minimum structure following the reaction coordinate past the second transition state and are not necessarily the lowest energy conformer. The structures of the products are also depicted in the Supporting Information.

For the investigated PPE derivatives, we found that the phenyl migration proceeds not through a single transition state but an oxaspiro[2.5]octadienyl radical intermediate (see Figure 1), characterized as a minimum on the potential energy surface. This is in accordance with recent computational results on the neophyl-like rearrangement in 1,1-diarylalkoxyl radicals.[28,29] Reaction 4 is similar (there is an additional aliphatic carbon in the ether bridge) to the reverse reaction of the 1,2-migration in the 1,1-diphenylethoxyl radical, for which an intermediate has also been predicted.[28,29] For a reaction to occur, the aromatic carbon adjacent to the ether oxygen has to approach the β-carbon radical center. There are multiple possibilities for this conformational change leading to three to five distinct reaction channels for each PPE derivative. We define a reaction channel as the process of conversion from reactant to product for a particular PPE derivative through an intermediate of unique conformation. Along a particular reaction channel conformational changes in the β-radical lead to a shallow minimum, which we will call prestructure throughout the paper. Movement of the aromatic and β-carbons toward each other yields the first transition state, where the carbon−carbon bond starts to form. The next step along the reaction coordinate is the intermediate, where an epoxy group is established. The oxygen−aromatic carbon bond in the epoxy group is then partially broken, yielding the second transition state. Finally, the products are formed, where the radical center has switched to the oxygen atom.

We located three reaction channels for the phenyl migration in the β-radical of PPE (**1**). The corresponding prestructures, first transition states, intermediates, and second transition states are shown in Figure 1. For the β-radicals of *p*HO-PPE (**2**), *p*CH_3O-PPE (**3**), PPE-*p*OCH_3 (**4**), PPE-*o*OCH_3 (**5**), and PPE-di-*o*OCH_3 (**6**) that information can be found in the Supporting Information. The prestructures were obtained by displacing along the imaginary mode in the first transition state and following the reaction

dx.doi.org/10.1021/jo2000385 |*J. Org. Chem.* 2011, 76, 2195–2203

Table 1. The 0 K Energies (in kcal/mol) of the Prestructures, First Transition States, Intermediates, and Second Transition States for the Phenyl Migration in the Derivatives Shown in Scheme 2 Relative to the Lowest Products of β-Hydrogen Abstraction (Reactants) with the Contribution of Each Channel to the Overall Rate Constant at 618 K (in %)[a]

		channel 1	channel 2	channel 3	channel 4	channel 5
β -PPE (**1**)	prestructure	0.56	0.32	1.12		
	TS1	20.46	19.81	18.38		
	intermediate	14.39	13.11	12.52		
	TS2	16.79	15.59	15.37		
	contribution	8.1	21.6	70.3		
β-*p*HO-PPE (**2**)	prestructure	0.67	0.49	1.12		
	TS1	20.36	19.76	18.29		
	intermediate	14.38	13.16	12.47		
	TS2	16.73	15.55	15.27		
	contribution	8.5	28.0	63.6		
β-*p*CH_3O-PPE (**3**)	prestructure	0.65	0.38	1.06		
	TS1	20.23	19.65	18.20		
	intermediate	14.22	13.02	12.32		
	TS2	16.69	15.44	15.21		
	contribution	9.0	21.3	69.8		
β-PPE-*p*OCH_3 (**4**)	prestructure	0.80	0.36	0.00		
	TS1	20.00	19.51	18.16		
	intermediate	12.64	11.26	10.67		
	TS2	14.35	13.10	12.98		
	contribution	18.5	31.1	50.4		
β-PPE-*o*OCH_3 (**5**)	prestructure	−1.03	−1.09	0.88	1.16	−1.08
	TS1	18.40	16.89	16.31	17.43	14.97
	intermediate	11.76	8.24	7.59	9.96	8.03
	TS2	15.27	11.31	11.00	12.56	12.82
	contribution	3.5	15.5	47.8	13.8	19.4
β-PPE-di-*o*OCH_3 (**6**)	prestructure	−3.12	−2.65	0.00	−1.62	
	TS1	15.60	14.58	13.72	12.41	
	intermediate	7.49	5.58	5.00	4.03	
	TS2	11.29	9.32	8.95	8.99	
	contribution	3.4	8.4	46.5	41.8	

[a] The contributions in % were obtained by taking the ratio of the steady-state rate constant for the individual channel and the total rate constant for the PPE derivative. All ratios are multiplied by 100.

coordinate toward reactants. In some cases, the prestructures coincided with the product of hydrogen abstraction, defined as reactant. The introduction of a hydroxy or methoxy substituent in the phenethyl group does not significantly change the structures of prestructures, transition states, and intermediates. Also, a methoxy substituent at the para-position of the phenyl ring adjacent to the ether oxygen has little effect on the geometries. In contrast, if a methoxy substituent is introduced at the ortho-position of the phenyl ring adjacent to the ether oxygen, the number of reaction channels increases. There are two distinct ortho-positions, which lead to distinct intermediates and transition states, whereas there is no distinction (aside from a substituent rotation) between the two sides of carbon−carbon approach in **1**, **2**, **3**, **4**, and **6**, resulting in a symmetry number of two per reaction channel for the latter derivatives. However, steric hindrance in the ortho-substituted derivative prevents some of the intermediates and transition states from forming stable conformers. For instance in **5**, we only located one of the two possible intermediates for channel 2 (see Figure 1: the conformer where the methoxy group points backward). If the methoxy group in **5** points forward in the intermediate of channel 3, the position of the phenyl rings adjusts, leading to a new conformer, where the phenyl rings are close to parallel to each other. The latter conformer was also found for the intermediate and transition states of **6**, producing an additional reaction channel for β-PPE-di-*o*OCH_3 compared to β-PPE.

In principle, the rotation of the substituents could also cause the emergence of distinct reaction channels. However, such rotation was not considered here for the following reasons: (1) the difference between the reaction barriers of the conformers of **2** in channel 1, where the hydroxy group points upward or downward, is smaller than 0.2 kcal/mol for either transition; (2) for **3**, the equivalent difference, where the methoxy group is rotated by 180°, does not exceed 0.05 kcal/mol; and (3) for **4**, where the *p*-methoxy substituent is located at the opposite phenyl ring, we tested the two conformers of channel 3, where methoxy either points forward or backward, the difference between the barriers for both transitions is smaller than 0.1 kcal/mol. The rotation of the methoxy group by 180° in **5** or **6** was not examined because the corresponding conformers in the parent molecules (prior to hydrogen abstraction) are not equilibrium structures.[24]

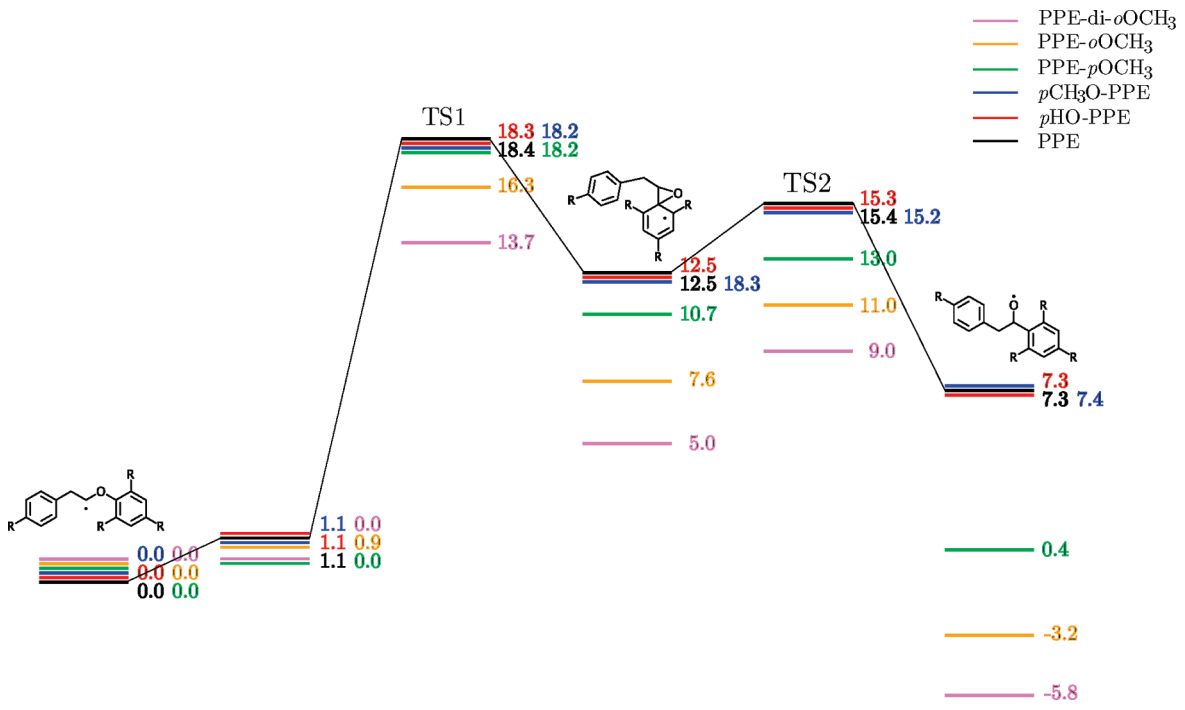

Figure 2. Reaction profiles for the reaction channels with the lowest first barrier for the phenyl-migration of PPE derivatives **1**−**6**, energy differences in kcal/mol. The first barrier is defined as the energy difference between the first transition state and prestructure.

Table 1 gives the 0 K energies of the prestructures, first transition states, intermediates, and second transition states for the phenyl migration in the derivatives shown in Scheme 2 relative to the lowest products of β-hydrogen abstraction (for their structures, see the Supporting Information). Some of the isolated prestructures in **5** and **6** are lower in energy than the β-radicals derived from the chain-like parent conformers. In these radicals, bending results in a conformer, where the *o*-methoxy group is close to the opposite phenyl ring, allowing for a stabilizing interaction. We observe that the first barrier is consistently higher than the second barrier; the first step is, therefore, the rate determining step in the phenyl-shift reaction. All channels listed in Table 1 are expected to significantly contribute to the overall rate constant. For PPE and derivatives **2**, **3**, and **4**, channel 3 has the lowest first barrier, suggesting that this will be the dominant reaction channel. Channels 5 and 4 contain the energetically lowest TS1 relative to the reactants for derivatives **5** and **6**, respectively. These channels correspond to sets of conformers where the phenyl rings of the channel 3 conformers for **1**−**4** are twisted toward a parallel position (see the Supporting Information). However, because of the stabilizing interaction in the prestructures relative to the reactants of channel 5 for derivative **5** and channel 4 for derivative **6**, which effectively increases the barriers, the lowest reaction barriers are again found for channel 3 of derivatives **5** and **6**, respectively.

The reaction profiles for the reaction channels with the lowest first barrier for the phenyl-migration of β-PPE derivatives **1**−**6** are depicted in Figure 2. We are able to make a rough comparison to published data on the rearrangement of 1,1-diphenylethoxyl radical:[29] the reported first barrier, intermediate energy, and second barrier are 9.9, 7.3, and 10.7 kcal/mol, respectively. The corresponding values in this work are the energies and barriers of the reverse reaction of the phenyl-shift in β-PPE, which are 8.1, 5.2, and 11.1 kcal/mol, respectively. The introduction of a *p*-methoxy group on both phenyl rings in the 1,1-diphenylethoxyl radical causes the second barrier to increase by 1.2 kcal/mol (first barrier and intermediate stay approximately constant).[28,29] In contrast, the introduction of a *p*-methoxy group on either phenyl ring of PPE (**3** and **4**) does not significantly affect the energy of the second transition state for the reverse phenyl shift compared to β-PPE. However, the energies of the intermediate and first (reverse) transition state are lowered in **4**, effectively increasing the barrier of the reverse second transition by 1.6 kcal/mol.

In Figure 2, we observe that neither a hydroxy nor a methoxy group at the para-position of the phenyl ring furthest from the radical center (derivatives **2** and **3**) influences the reaction profile significantly when compared to β-PPE. If a *p*-methoxy group is introduced in the phenyl ring closest to the radical center (derivative **4**), the first reaction barrier is little altered, but we see a reduction of the intermediate energy, the second barrier, and the product energy by 1.8, 2.4, and 6.9 kcal/mol, respectively. An ortho-substituent (derivative **5**) reduces the first barrier by 2.1 kcal/mol and further decreases intermediate, second transition state, and product energies by 3.1, 2.0, and 3.6 kcal/mol compared to derivative **4**. This effect is approximately doubled when a second *o*-methoxy group is included in the phenyl ring adjacent to the ether oxygen (derivative **6**). This can partially be explained by looking at the spin density along the reaction coordinate.

As an example, Figure 3 shows the spin densities for channel 3 of the phenyl migration in **5**. In the reactant and prestructure most spin density is localized at the β-carbon, which comprises the radical center. As the carbon−carbon bond is formed in the first transition state, spin density shifts toward the phenyl ring adjacent to the ether oxygen, which is connected to the radical center by the partially formed bond. In the epoxy intermediate, the spin density seems nearly evenly distributed between epoxy and the phenyl ring. Further along the reaction coordinate, the spin density on the epoxy oxygen is growing, while spin density

dx.doi.org/10.1021/jo2000385 |*J. Org. Chem.* 2011, 76, 2195–2203

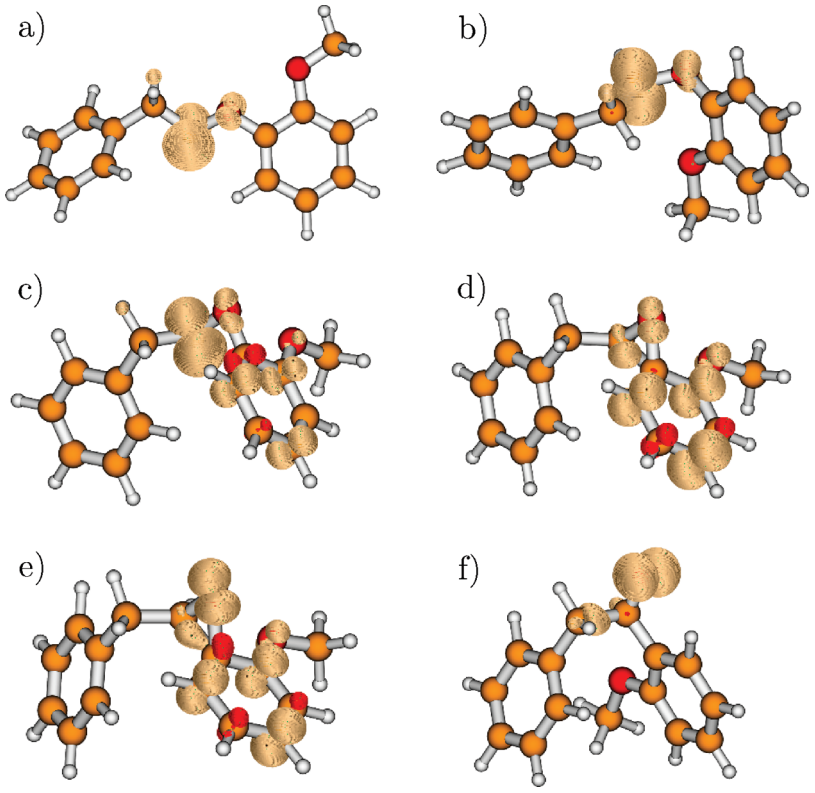

Figure 3. Spin densities along the reaction coordinate of channel three of the phenyl migration in **5**: (a) reactant, (b) prestructure, (c) first transition state, (d) intermediate, (e) second transition state, and (f) product.

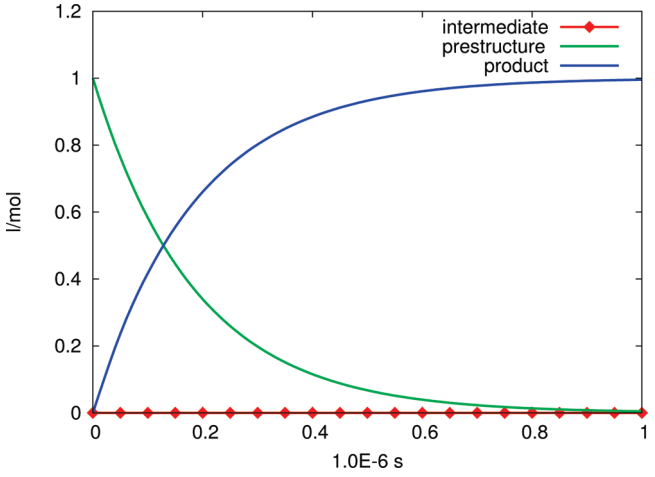

Figure 4. Concentration of prestructure, intermediate, and product as a function of time for channel three of the phenyl-migration reaction in β-PPE, temperature 618 K.

remains in the phenyl ring in the second transition state. In the final product, the spin density is concentrated on the oxygen, which has become the radical center. Spin delocalization into the phenyl ring is most pronounced for the intermediate and the second transition state. Methoxy substituents located at the phenyl ring adjacent to the ether oxygen participate in spin delocalization, as is evident from Figure 3c−e, and their stabilizing influence is, therefore, most pronounced in the intermediate and the second transition state. We also saw an energy decrease for the intermediates and second transition states for derivatives **4**−**6** in the reaction profile. In contrast, methoxy substituents on the opposite ring cannot aid spin delocalization. Substituents on either ring do not participate in spin delocalization in the products and spin delocalization cannot explain product stabilization. However, the product geometries for **5** and **6** indicate that the *o*-methoxy group stabilizes the products through interaction with the opposite phenyl ring (see the Supporting Information for product structures).

Table 1 shows that the prestructures are at most 1.2 kcal/mol higher in energy than the reactants. The prestructures are related through conformational changes and we assume that they are in thermal equilibrium. The rate constants to form the intermediates only depend on the energy differences between the first transition states and the prestructures. The overall rate constant of the phenyl migration is the rate constant of a series of first-order reactions, where the reverse reaction from intermediate to prestructure is considered. Applying the steady-state approximation to the intermediate, the rate constant for the phenyl migration is given by

$$k = \frac{k_1 k_2}{(k_{-1} + k_2)} \qquad \text{(I)}$$

where k_1 is the forward rate constant for the reaction from prestructure to intermediate (reaction 1), k_{-1} is the reverse rate constant from intermediate to prestructure (reaction −1), and k_2 is the forward rate constant from intermediate to product (reaction 2). To test the validity of the steady state approximation, we solved the differential equations for reactions 1, −1, and 2 numerically for β-PPE. Figure 4 contains the plot of the concentration of the prestructure, intermediate, and product as a

dx.doi.org/10.1021/jo2000385 |*J. Org. Chem.* 2011, 76, 2195–2203

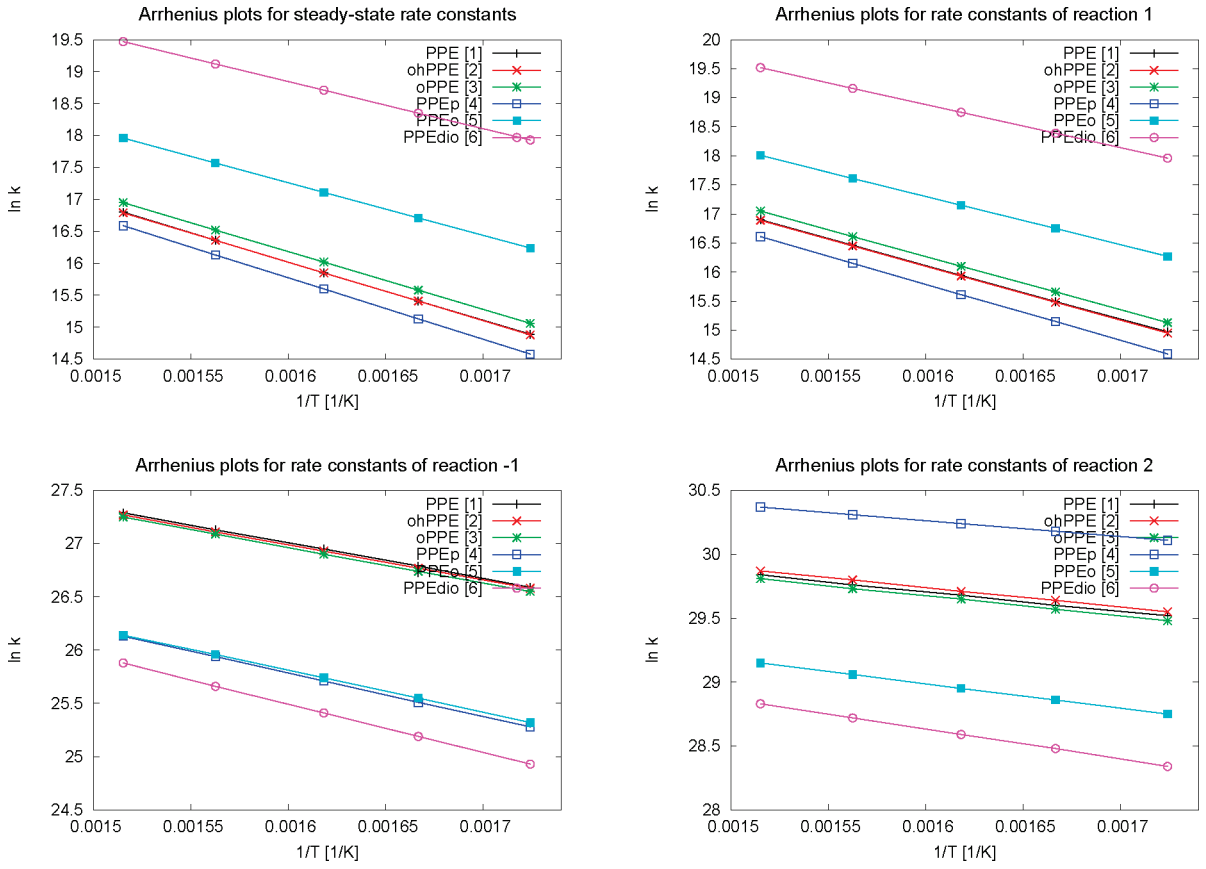

Figure 5. Arrhenius plots for the phenyl migration in **1**−**6**: steady-state rate constant, forward rate constant from prestructure to intermediate (reaction 1), reverse rate constant from intermediate to prestructure (reaction −1), forward rate constant from intermediate to product (reaction 2); temperature range 580−660 K.

function of time for channel 3 of the phenyl-migration reaction in β-PPE. We observe that the concentration of the intermediate remains close to the *x*-axis (very low) through the entire reaction, indicating that the steady-state approximation is valid. Since the character of the migration reaction changes with the substituents, we repeated the test for channel 3 of the rearrangement in β-PPE-di-*o*OCH_3. For derivative **6**, the second barrier is 2.1 kcal/mol larger than the corresponding barrier for PPE, suggesting a higher intermediate concentration. However, we, again, observed that the intermediate concentration remains low and the steady-state approximation is valid. The corresponding plot can be found in the Supporting Information.

We calculated the elementary rate constants for reactions 1, −1, and 2 for β-PPE and β-PPE derivatives **2**−**6**, including all reaction channels listed in Table 1. A symmetry number of two is assigned to each reaction channel for **1**−**4** and **6**, the reaction channels of **5** have weight factors of one. The steady-state rate constants are computed by using eq I. Table 1 includes the contribution of each channel to the total rate constant at 618 K. Channel 3 contributes the most for all derivatives and is, with more than 60%, dominant for derivatives **1**−**3**. Its participation is reduced to about 50% for derivatives **4**−**6**. Channel 2, with about 30%, becomes competitive for the phenyl-shift reaction in β-PPE-*p*OCH_3 (**4**), and the contribution of channel 4 is comparative for β-PPE-di-*o*OCH_3 (**6**).

Figure 5 shows the Arrhenius plots for the elementary reactions and the steady-state rate constants of the phenyl migration in the β-radicals. Table 2 summarizes the overall activation

Table 2. Activation Energies (in kcal/mol) and Pre-Factors Derived from the Arrhenius Plots of the Steady-State Rate Constants in Figure [5], Temperature Range 580−660 K, and Relative Rate Constants at 618 K

	ln *A*	E_A	$k_x/k_{\beta\text{-PPE}}$[a]
β-PPE	30.6	18.1	1.0
β-*p*HO-PPE	30.6	18.2	1.0
β-*p*CH_3O-PPE	30.7	18.0	1.2
β-PPE-*p*OCH_3	31.1	19.1	0.8
β-PPE-*o*OCH_3	30.5	16.4	3.5
β-PPE-di-*o*OCH_3	30.6	14.6	17.3

[a] x refers to the derivative listed in the first column.

energies, prefactors, and relative rate constants at 618 K. We observe that the overall rate constant is dominated by the rate constant for reaction 1: absolute values are only slightly reduced compared to reaction 1 and substituent effects in the overall rate constants parallel the substituent effects in the rate constants of reaction 1. A substituent on the phenyl ring in the phenethyl group and the *p*-methoxy substituent on the phenyl ring adjacent to the ether oxygen alter the overall rate constant only slightly. The small decrease in the rate constant for the phenyl shift in β-PPE-*p*OCH_3 (**4**) compared to β-PPE (**1**), β-*p*HO-PPE (**2**), and β-*p*CH_3O-PPE (**3**) is due to the prestructures, which were localized for **1**, **2**, and **3**, effectively lowering the barrier of the first transition. For **4**, displacement along the imaginary mode in the

dx.doi.org/10.1021/jo2000385 |*J. Org. Chem.* 2011, 76, 2195–2203

first transition state of the dominant reaction channel 3 and following the reaction coordinate led to the reactant without passing a minimum structure. The *o*-methoxy substituent on the phenyl ring adjacent to the ether oxygen and, to a larger extent the di-*o*-methoxy substituents, accelerates the rate of the phenyl migration (by a factor of 3.5 and 17.3, respectively), again in correspondence with the increased rate constants of reaction 1. The *o*- and di-*o*-methoxy substituents have an opposite effect on the rate of reactions −1 and 2, which are decelerated, but do not sufficiently influence the overall rate constant to be consequential. The *p*-methoxy substituent on the phenyl ring adjacent to the ether oxygen has a small effect on the rate constant of reaction 1, decreases the rate constant for reaction −1, and increases the rate constant for reaction 2, showing how the influence of the substituent grows stronger as the reaction proceeds. The acceleration of reaction 2 is the consequence of a lowered intermediate energy compared to β-PPE; the energy is even more lowered in the second transition state, consequently reducing the second energy barrier.

As described in the Introduction, if the rate constant for the phenyl shift reaction is not fast, then intermolecular hydrogen transfer could become competitive, converting β-radicals into α-radicals and altering the α/β-product selectivity in the pyrolysis of PPE. In the earlier pyrolysis investigations, we observed that the α/β-selectivity did not depend on the PPE concentration, suggesting that the intermolecular hydrogen transfer was not competitive even at the highest concentration in the neat liquid (3.8 M).[14] Using thermochemical kinetic analysis, we estimated that this lack of concentration dependence required the phenyl shift rate constant to be larger than 4.0×10^5 s^{-1} at 648 K.[14] Using the Arrhenius parameters for PPE in Table 2, we calculate that the phenyl shift rate constant at 648 K is 1.6×10^7 s^{-1}, consistent with experiment.

3. CONCLUSIONS

We investigated the effects of naturally occurring substituents on the phenyl-migration reaction in the β-phenethyl phenyl ether radical. The β-radicals are formed by hydrogen abstraction during pyrolysis and undergo conformational changes leading to prestructures for the phenyl-shift reaction. The latter proceeds through a first transition state yielding an intermediate, which further reacts through a second transition state to the products, where the radical center has shifted from a carbon to an oxygen atom. We calculated the rate constant of the elementary reactions from prestructure to intermediate, the reverse reaction from intermediate to prestructure, and from intermediate to product. We applied the steady-state approximation to compute overall rate constants of the phenyl-shift reaction. The applicability of the steady-state approximation was confirmed by numerical solution of the rate equations of the elementary steps for two PPE derivatives and the observation that the concentration of the intermediates remained small during the reaction. We found that the overall rate constant is dominated by the rate constant of the reaction from prestructure to intermediate.

Substituents on the phenyl ring of the phenethyl group have little influence on the overall rate constant as well as on the rate constants of the elementary reactions. Transition states and intermediates are stabilized by spin delocalization involving the phenyl ring adjacent to the ether oxygen and substituents located there have a potentially larger effect on the reaction. If the phenyl ring adjacent to the ether oxygen carries a *p*-methoxy substituent, the energies of the intermediate, second transition state, and product are lowered compared to that for β-PPE. However, due to the dominance of the rate constant involving the first transition state, the overall rate constant for the phenyl migration is similar to that for β-PPE. Accelerated rates, by a factor of 3.5 at 618 K, were obtained with *o*-methoxy substituents on the phenyl ring adjacent to the ether oxygen. The increase in the overall rate was larger when di-*o*-methoxy substituents were introduced; we computed a factor of 17.3 compared to β-PPE.

4. COMPUTATIONAL DETAILS

All electronic structure calculations were carried out with the NWChem program package.[31] We used density functional theory, specifically, the M06-2X kinetic functional,[30] to explore the potential energy surfaces. We chose the NWChem "xfine" integration grid, therefore avoiding inaccuracies due to the grid size.[32] Geometry optimizations and frequency calculations were performed with a mixed basis set based on the 6-31G* basis set including diffuse functions where the unpaired electron is located; i.e., the atoms of the epoxide ring in the intermediates and transition states and the radical centers in reactants and product carried a 6-31++G** basis set. Intermediates, prestructures, and transition states were confirmed by frequency analysis. Energies at stationary points were computed with the 6-311++G** basis set and 0 K energy differences were zero-point corrected.

Reaction channels were identified by first searching for intermediates with distinct conformation. Derivatives **1**, **2**, **3**, **4**, and **6** have two identical sides of carbon−carbon approach (aside from substituent rotation) and we employed four starting structures with different orientations of the benzyl group to the epoxy group. The phenyl ring, where one carbon atom is part of the epoxy group, does not have rotational freedom. Derivative **5** contains a methoxy substituent in the ortho position, which lifts the symmetry in the intermediate. We, therefore, used eight starting structures instead of four. Geometry optimizations led to the intermediates described in the section above. We then located the transition states based on the intermediates. The first transition states were obtained by elongating the carbon−carbon distance in the epoxy group of the intermediate and launching a saddle point search; the second transition states were identified by extending the oxygen−aromatic carbon distance in the epoxy group followed by a saddle point search.

Rate constants for elementary reactions were calculated with our own Python code, which is interfaced to the NWChem program package. We applied transition state theory[33] and included a Wigner tunneling correction[34] to compute unimolecular reaction rate constants. Rate constants calculated within transition state theory are pressure independent; pressure-dependent studies have not been conducted within the present work. Anharmonic effects were incorporated for low-frequency vibrations up to 110 cm^{-1}, which corresponds to about 5 modes per transition state, intermediate, and reactant. Within the independent mode approximation, the anharmonic potentials were obtained by displacement along the normal modes and 9 energy points per mode were used for a fourth-order polynomial fit. The anharmonic vibrational partition functions were computed with the semiclassical Wigner−Kirkwood approximation, as outlined in ref 22.

We used Mathematica[35] for the numerical integration of rate equations.

■ ASSOCIATED CONTENT

Supporting Information. Reactant and product structures for derivatives **1**−**6**, prestructures, first transition states, intermediates, and second transition states of the phenyl migration in **2**−**6**, the concentration plot for the phenyl migration in β-PPE-di-*o*OCH_3 (channel 3), and Cartesian coordinates, the total energies, the zero point energies, and the number of imaginary

frequencies for all calculated structures mentioned in the text. This material is available free of charge via the Internet at http://pubs.acs.org.

AUTHOR INFORMATION

Corresponding Author

*To whom correspondence should be addressed. E-mail: bestea@ornl.gov. Phone: 865-241-3160. Fax: 865-574-0680.

ACKNOWLEDGMENT

We would like to thank Jarod M. Younker for his assistance. This research was sponsored by the Division of Chemical Sciences, Geosciences, and Biosciences, Office of Basic Energy Sciences, U.S. Department of Energy and was performed in part using the resources of the Center for Computational Sciences at Oak Ridge National Laboratory under contract DE-AC05-00OR22725. It was also supported by an allocation of advanced computing resources provided by the National Science Foundation; computations were performed on Kraken at the National Institute for Computational Sciences (http://www.nics.tennessee.edu/).

REFERENCES

(1) Mohan, D.; Pittman, C. U., Jr.; Steele, P. H. *Energy Fuels* **2006**, *20*, 848–889.
(2) Petrou, E. C.; Pappis, C. P. *Energy Fuels* **2009**, *23*, 1055–1066.
(3) Stöcker, M. *Angew. Chem., Int. Ed.* **2008**, *47*, 9200–9211.
(4) Chheda, J. N.; Huber, G. W.; Dumesic, J. A. *Angew. Chem., Int. Ed.* **2007**, *46*, 7164–7183.
(5) Czernik, S.; Bridgewater, A. V. *Energy Fuels* **2004**, *18*, 590–598.
(6) Huber, G. W.; Iborra, S.; Corma, A. *Chem. Rev.* **2006**, *106*, 4044–4098.
(7) Kawamoto, H.; Ryoritani, M.; Saka, S. *J. Anal. Appl. Pyrolysis* **2008**, *81*, 88–94.
(8) Kidder, M. K.; Britt, P. F.; Chaffee, A. L.; Buchanan, A. C., III *Chem. Commun.* **2007**, *1*, 52–54.
(9) Kandanarachchi, P. H.; Autrey, T.; Franz, J. A. *J. Org. Chem.* **2002**, *67*, 7937–7945.
(10) Kuroda, K.-i. *J. Anal. Appl. Pyrolysis* **1995**, *35*, 53–60.
(11) Autrey, S. T.; Alnajjar, M. S.; Nelson, D. A.; Franz, J. A. *J. Org. Chem.* **1991**, *56*, 2197–2202.
(12) Klein, M. T.; Virk, P. S. *Ind. Eng. Chem. Fundam.* **1983**, *22*, 35–45.
(13) Gilbert, K. E.; Gajewski, J. J. *J. Org. Chem.* **1982**, *47*, 4899–4902.
(14) Britt, P. F.; Buchanan, A. C., III; Malcolm, E. A. *J. Org. Chem.* **1995**, *60*, 6523–6536.
(15) Britt, P. F.; Kidder, M. K.; Buchanan, A. C., III *Energy Fuels* **2007**, *21*, 3102–3108.
(16) Martinez, C.; Rivera, J. L.; Herrera, R.; Rico, J. L.; Flores, N.; Rutiaga, J. G.; López, P. *J. Mol. Model* **2008**, *14*, 77–91.
(17) Durbeej, B.; Wang, Y.-N.; Eriksson, L. A. *Lecture notes in computer science*; Springer-Verlag: Berlin, Germany, 2003; pp 137−165.
(18) Elder, T. *Holzforschung* **2010**, *64*, 435–440.
(19) Agache, C.; Popa, V. I. *Monatsh. Chem.* **2006**, *137*, 55–68.
(20) da Silva, G.; Bozzelli, J. W. *J. Phys. Chem. A* **2007**, *111*, 7987–7994.
(21) Beste, A.; Buchanan, A. C., III *J. Org. Chem.* **2009**, *74*, 2837–2841.
(22) Beste, A.; Buchanan, A. C., III; Britt, P. F.; Hathorn, B. C.; Harrison, R. J. *J. Phys. Chem. A* **2007**, *111*, 12118–12126.
(23) Beste, A.; Buchanan, A. C., III; Harrison, R. J. *J. Chem. Phys. A* **2008**, *112*, 4982–4988.
(24) Beste, A.; Buchanan, A. C., III *Energy Fuels* **2010**, *24*, 2857–2867.
(25) Falvey, D. E.; Khambatta, B. S.; Schuster, G. B. *J. Phys. Chem.* **1990**, *94*, 1056–1059.
(26) Grossi, L.; Strazzari, S. *J. Org. Chem.* **2000**, *65*, 2748–2754.
(27) Antunes, C. S. A.; Bietti, M.; Ercolani, G.; Lanzalunga, O.; Salamone, M. *J. Org. Chem.* **2005**, *70*, 3884–3891.
(28) Bietti, M.; Ercolani, G.; Salamone, M. *J. Org. Chem.* **2007**, *72*, 4515–4519.
(29) Smeu, M.; DiLabio, G. *J. Org. Chem.* **2007**, *72*, 4520–4523.
(30) Zhao, Y.; Truhlar, D. G. *Acc. Chem. Res.* **2008**, *41*, 157.
(31) Valiev, M.; Bylaska, E.; Govind, N.; Kowalski, K.; Straatsma, T.; van Dam, H.; Wang, D.; Nieplocha, J.; Apra, E.; Windus, T.; de Jong, W. *Comput. Phys. Commun.* **2010**, *181*, 1477.
(32) Wheeler, S. E.; Houk, K. N. *J. Chem. Theory Comput.* **2010**, *6*, 395–404.
(33) Holbrook, K. A.; Piling, M. J.; Robertson, S. H. *Unimolecular reactions*, 2nd ed.; John Wiley & Sons: Chichester, England, 1996.
(34) Henriksen, N. E.; Hansen, F. Y. *Theories of molecular reaction dynamics: The microscopic foundation of chemical kinetics*; Oxford University Press Inc.: New York, 2008.
(35) *Mathematica*, Version 7.0; Wolfram Research, Inc., Champaign, IL, 2008.